THE FAR FIELD DIFFRACTION PATTERN FOR CORNER REFLECTORS WITH COMPLEX REFLECTION COEFFICIENTS

R. F. Chang, D. G. Currie, and C. O. Alley

Department of Physics and Astronomy
University of Maryland
College Park, Maryland

and

M. E. Pittman

Department of Physics
Louisiana State University
New Orleans, Louisiana

Technical Report 70-104

April 1970

UNIVERSITY OF MARYLAND
DEPARTMENT OF PHYSICS AND ASTRONOMY
COLLEGE PARK, MARYLAND

THE FAR FIELD DIFFRACTION PATTERN FOR CORNER REFLECTORS WITH COMPLEX REFLECTION COEFFICIENTS*

R. F. Chang, D. G. Currie, and C. O. Alley

Department of Physics and Astronomy
University of Maryland
College Park, Maryland

and

M. E. Pittman

Department of Physics
Louisiana State University
New Orleans, Louisiana

Technical Report 70-104

April 1970

* This work was supported by NASA Grants NGR 21-002-109 and NAS 9-7809, and The University of Maryland Computer Science Center under NASA Grant NsG-398. Grant NsG-398.

ABSTRACT

The far field diffraction pattern of a geometrically perfect corner reflector is examined analytically for normally incident monochromatic light. The states of polarization and the complex amplitudes of the emerging light are expressed through transformation matrices in terms of those of the original incident light for each sextant of the face in a single coordinate system. The analytic expression of the total diffraction pattern is obtained for a circular face. This expression consists of three component functions in addition to the basic Airy function. The coefficient of each function is expressed in terms of complex coefficients of reflectance of the reflecting surface. Some numerical results for different reflecting surfaces, including total internal reflection, are presented. The iso-intensity contours of the diffraction pattern evaluated from the analytical expressions for an uncoated solid corner reflector are also presented along with the photographs of the pattern.

INDEX HEADINGS: Diffraction, Corner Reflector.
Total Internal Reflection.
Polarization Effects.

I. INTRODUCTION

It is known that a monochomatic plane wave of light falling normally upon a flat circular mirror produces in the far field, upon reflection, the well-known Airy diffraction pattern. When the flat mirror is replaced by a corner reflector of the same circular aperture the far field pattern is no longer the Airy pattern. We will consider, in this report, the far field diffraction pattern of a corner reflector with special emphasis on the effects of the relative phase shifts between orthogonal polarizations caused by total internal reflection. Mahan[1] has reported a similar comprehensive study on the polarization effects from a roof prism.

E. R. Peck[2] has studied the resultant state of polarization of the reflected light when a pencil of light falls upon one sector of a corner reflector. M. M. Rao[3], following the method of Peck, has made a numerical study of the state of polarization for a corner reflector constructed of a particular type of glass. The eigen states of polarization predicted by Peck have been experimentally verified by Rabinowitz, et al[4]. A study, in terms of geometric optics, of the effects of angular errors in the prism on the return image has been made by P. R. Yoder, Jr.[5], and also by R. C. Spencer[6]. However, our present discussion shall assume that the corner is geometrically perfect; i.e. there are no angular erros in the corner reflector.

In the following we consider the far field pattern produced by combining the beams of different polarization which emerge from the six sectors of the corner reflector. The polarization and amplitude of each of these six beams is determined by the optical properties of the reflection surface. The reflection surface can be one of many forms, such as air to metal, glass to metal and glass to air for the case of an open corner, a solid corner with metal coating, and an uncoated solid corner,

respectively. In general, this pattern has more structure and angular divergence than the pattern which would be obtained if the corner reflector acted in the same manner as a flat mirror of the same diameter.

In more detail, each ray which "composes" the incident plane wave falling on a corner reflector is followed through the corner reflector in the manner of Peck, and the phase and amplitude of the ray emerging from the face of the corner reflector are determined. We thus neglect diffraction effects which occur inside the corner reflector. The phase shift and amplitude are determined by the optical properties of the rear surface; i.e., the glass-metal, glass-air, or air-metal interface. Each of these rear interfaces causes a relative phase shift between the components polarized parallel and perpendicular to the plane of incidence. An interface with a metal component also introduces a change in the amplitude of the light wave. Our results will be compared to those for a "perfect" metal coating at the rear interface by which we mean an interface with the ideal properties of no change in amplitude and a relative change of phase between the parallel and perpendicular components of polarization of $-\pi$. (A material with infinite conductivity at optical frequencies would satisfy this criterion of "perfection.")

The amplitude and phase or, equivalently, the complex amplitudes thus determined have different values on the different sextants. In this computation, it has been assumed that the incident plane wave is perpendicular to the front face. Tilting the corner reflector by an angle ϕ would have two effects: (1) an overall change in the apparent shape of the front face (or the aperture) which would expand one axis of the resultant diffraction pattern, and (2) a change in the angles of refraction at the rear interface, which would involve the change of relative phase shifts with angle. The latter effect is second order in the angle

ϕ and thus small for small angles. For a larger angle, the analytic expression of the complex amplitude of the emerging beam cannot be obtained simply. We have, utilizing a computer, adopted the ray trace technique and we will report the results separately.

The face of the corner reflector is assumed to be circular. Scalar diffraction theory is used to determine the far field pattern which results from all sextants with different complex amplitudes. The diffraction is calculated first for an arbitrary complex amplitude for each sector, and later the complex amplitudes are given the values which would result from a particular rear interface. The Fresnel reflection from the front face has been neglected at present as we may assume an anti-reflection coating on the front face of a corner reflector. The presence of the Fresnel reflection at the front face causes multiple reflections which interfere with the original retro beam. We will present a detailed discussion of this aspect separately.

The properties of specific interfaces are considered in Section V, and the diffraction patterns for silver, aluminum and total internal reflection are discussed. The metals have diffraction patterns rather similar to that of a "perfect" metal, and total internal reflection produces marked diffraction effects. The iso-intensity contours, which are evaluated from the analytic expressions, of the diffraction pattern for an uncoated solid corner reflector are presented along with the photographs of the pattern.

The analysis was undertaken to provide a thorough understanding of the diffraction pattern of corner reflectors in connection with the design and testing of the Apollo 11 Laser Ranging Retro-Reflector. This uses total internal reflection to allow near diffraction limited operation in the lunar thermal environment.[7]

II. POLARIZATION AND INTENSITY EFFECTS OF A CORNER REFLECTOR ON A PENCIL OF LIGHT

The front face of a corner reflector is divided into six equal sections, when viewed from the front, by the projections of the three real back edges and their images. We define a coordinate system in the face of the corner reflector by a pair of mutually orthogonal unit vectors $\hat{i}$ and $\hat{j}$ with the $\hat{j}$-axis coincident with the projection of one of the real back edges in the face as shown in Fig. 1. The six sections are labeled by numbers 1 through 6. A beam of light entering the corner reflector through one of the sections always emerges from the opposite section.

If we consider a pencil of light which enters axially into the sextant labeled by 4 then the unit vectors $\hat{i}$ and $\hat{j}$ are perpendicular and parallel respectively to this plane of incidence. We assume here the light to be monochromatic and of single polarization. The amplitude of the light entering the 4th sextant can then be represented by $\underset{\sim}{u}$ which has two complex components u_1 and u_2 in the directions $\hat{i}$ and $\hat{j}$. This light beam, after being reflected consecutively from three back surfaces, emerges from the sextant labeled by 1 with amplitude $\underset{\sim}{v}$ which is different from $\underset{\sim}{u}$. By tracing the light through each reflection, it has been found[1] that $\underset{\sim}{u}$ and $\underset{\sim}{v}$ can be related by a 2 x 2 matrix $\underset{\sim}{C}$, such that $v_i = \sum_{j=1}^{2} C_{ij} u_j$, $i = 1,2$ or $\underset{\sim}{v} = \underset{\sim}{C}\underset{\sim}{u}$.

The matrix $\underset{\sim}{C}$ has the form

$$C_{11} = \frac{1}{8} r_s \left[(r_s + r_p)^2 + 4 r_p (r_s - r_p) \right] \tag{1a}$$

$$C_{12} = \frac{\sqrt{3}}{8} r_p (r_s + r_p)^2 \tag{1b}$$

$$C_{21} = \frac{\sqrt{3}}{8} r_s (r_s + r_p)^2 \tag{1c}$$

$$C_{22} = \frac{1}{8} r_p \left[4r_s (r_s - r_p) - (r_s + r_p)^2\right]. \tag{1d}$$

where r_s and r_p are complex coefficients of reflectance which may be written as $r_s = \rho_s \exp(i\delta_s)$ and $r_p = \rho_p \exp(i\delta_p)$. For lossless reflection ρ_s and ρ_p have unit magnitude. In general, however, the magnitudes of ρ_s and ρ_p are less than unity, representing the losses in reflection. This is the matrix for light emerging from the first sextant and the matrix in Eq. (1) could be labeled $\underset{\sim}{C}^1$. In general, the transformation matrix or the relation between incident intensity and polarization is different for each sextant, so we have

$$\underset{\sim}{v}^n = \underset{\sim}{C}^n \underset{\sim}{u}$$

where n = 1, 2, 3, 4, 5, and 6. The superscript n of the complex amplitude $\underset{\sim}{v}^n$ and the matrix $\underset{\sim}{C}^n$ is associated with the light emerging from the nth sextant. The matrix in Eq. (1), now identified as $\underset{\sim}{C}^1$ can be re-expressed in terms of Pauli's spin matrices, for the convenience of the following calculation, in the form

$$\underset{\sim}{C}^1 = \xi \underset{\sim}{1} + \eta\sqrt{3/2}\,\underset{\sim}{\sigma}_x + \zeta\underset{\sim}{\sigma}_y + \eta\sqrt{1/2}\,\underset{\sim}{\sigma}_z$$

where

$$\underset{\sim}{1} = \begin{pmatrix} 1 & 0 \\ 0 & 1 \end{pmatrix}, \quad \underset{\sim}{\sigma}_x = \begin{pmatrix} 0 & 1 \\ 1 & 0 \end{pmatrix}, \quad \underset{\sim}{\sigma}_y = \begin{pmatrix} 0 & -i \\ i & 0 \end{pmatrix}, \quad \underset{\sim}{\sigma}_z = \begin{pmatrix} 1 & 0 \\ 0 & -1 \end{pmatrix}$$

and

$$\xi = \frac{1}{16} (r_s - r_p) \left[3(r_s + r_p)^2 - 2(r_s - r_p)^2\right], \tag{2a}$$

$$\eta = \frac{\sqrt{2}}{16} (r_s + r_p)^3, \tag{2b}$$

$$\zeta = -i \frac{\sqrt{3}}{16} (r_s + r_p)^2 (r_s - r_p). \tag{2c}$$

The 3rd and the 5th sextants transform into the first sextant if we rotate the coordinates by $\pm 120°$, therefore one can obtain the matrices $\underset{\sim}{C}^3$ and $\underset{\sim}{C}^5$ through the rotation of the coordinate system. Such a rotation may be accomplished by $\underset{\sim}{R}^{-1}\ \underset{\sim}{C}\ \underset{\sim}{R}$, where $\underset{\sim}{R} = -\frac{1}{2}(\underset{\sim}{1} - \sqrt{3}\ i\ \underset{\sim}{\sigma}_y)$ for $+120°$ and $\underset{\sim}{R} = -\frac{1}{2}(\underset{\sim}{1} + \sqrt{3}\ i\ \underset{\sim}{\sigma}_y)$ for $-120°$, yielding

$$\underset{\sim}{C}^3 = \xi\underset{\sim}{1} - \sqrt{3/2}\eta\underset{\sim}{\sigma}_x + \zeta\underset{\sim}{\sigma}_y + \sqrt{1/2}\eta\underset{\sim}{\sigma}_z ,$$

$$\underset{\sim}{C}^5 = \xi\underset{\sim}{1} + \zeta\underset{\sim}{\sigma}_y - \sqrt{2}\eta\underset{\sim}{\sigma}_z .$$

Matrices $\underset{\sim}{C}^2$, $\underset{\sim}{C}^4$, and $\underset{\sim}{C}^6$ can be obtained by inverting $\underset{\sim}{C}^5$, $\underset{\sim}{C}^3$, and $\underset{\sim}{C}^1$ respectively with σ_z because they are mirror image pairs and we obtain

$$\underset{\sim}{C}^n = \underset{\sim}{\sigma}_z \underset{\sim}{C}^{7-n} \underset{\sim}{\sigma}_z, \quad n = 2,\ 4,\ \text{and}\ 6 .$$

This equation, because of the anticommutation relation of σ's, results in simply changing of signs of the coefficients of σ_x and σ_y components. Consequently we can write $\underset{\sim}{C}^n$ in a general form as

$$\underset{\sim}{C}^n = \xi\underset{\sim}{1} + f_n\sqrt{3/2}\eta\underset{\sim}{\sigma}_x + g_n\zeta\underset{\sim}{\sigma}_y + h_n\sqrt{1/2}\eta\underset{\sim}{\sigma}_z . \qquad (3)$$

The coefficients f_n, g_n and h_n are tabulated in Table I for all sextants.

As indicated by the form of the transformation matrices $\underset{\sim}{C}^n$ the polarization and amplitude of the entering light is in general not preserved. One can, however, use projection operators to decompose the emerging beam into two polarization components along directions other than $\hat{i}$ and $\hat{j}$. In particular we will consider one component parallel to the incident polarization and the other perpendicular to it. Assume the

incident light to be linearly polarized with the direction of the electric field at an angle θ to the $\hat{i}$-axis so it has the form $\underset{\sim}{u} = u_o \begin{pmatrix} \cos\theta \\ \sin\theta \end{pmatrix}$ where u_o is the amplitude of the field. The eigenvectors of these projection operators are,

$$v_p = \begin{pmatrix} \cos\ \theta \\ \sin\ \theta \end{pmatrix} \text{ and } v_s = \begin{pmatrix} \sin\ \theta \\ -\cos\ \theta \end{pmatrix}$$

respectively for the components parallel and perpendicular to the incident polarization. Thus the normalized complex amplitudes of the emerging light from nth sextant for these two components are,

$$\gamma_p^n \equiv \underset{\sim}{v}_p^{\dagger}\ \underset{\sim}{\underset{\sim}{C}}^n\ \underset{\sim}{u}/(\underset{\sim}{u}^{\dagger}\underset{\sim}{u})^{\frac{1}{2}}$$

$$= \xi + f_n\sqrt{3/2n}\ \sin(2\theta) + h_n\sqrt{1/2n}\ \cos\ (2\theta) \qquad (4a)$$

$$\gamma_s^n \equiv \underset{\sim}{v}_s\ \underset{\sim}{\underset{\sim}{C}}^n\ \underset{\sim}{u}/(\underset{\sim}{u}^{+}\underset{\sim}{u})^{\frac{1}{2}}$$

$$= -g_n i\zeta + h_n\sqrt{1/2n}\ \sin\ (2\theta) - f_n\sqrt{3/2n}\ \cos\ (2\theta) \qquad (4b)$$

It is now clear that the polarization and intensity of the emerging light are different from one sextant to the other and are also determined by the magnitudes and relative phase of γ_p^n and γ_s^n .

III. DIFFRACTION PATTERN FOR A SIX-SECTORED CIRCLE WITH ARBITRARY PHASES AND AMPLITUDES

For a single polarization the integral governing Fraunhofer diffraction for circular aperture of radius a is given, in polar coordinates, by[8]

$$U(P) = B \int_0^a \int_0^{2\pi} e^{-ik\rho w \cos(\phi-\psi)} \rho d\rho d\phi \qquad (5)$$

where U(P) is the amplitude at the far field point P, and (ρ,ϕ) is the polar coordinate at the aperture whereas (w,ψ) is the polar coordinate of the point P, and $k \equiv 2\pi/\lambda$. However, w is the sine of the angle between the direction of the light beam and the direction of point P. The constant B is the complex amplitude of the light in the aperture.

Now consider a circular aperture of radius a with imaginary lines dividing the aperture into six sextants. Suppose the linearly polarized light emerging from the aperture has different phases and amplitudes at different sextants but with uniform phase and amplitude over a given sextant. Then the diffraction integral should become

$$U(P) = \sum_{n=1}^{6} B_n \int_0^a \int_{(n-1)\pi/3}^{n\pi/3} e^{-ik\rho w \cos(\phi-\psi)} \rho d\rho d\phi , \qquad (6)$$

where B_n describes the phase and the amplitude of the light emerging from the n-th sextant. The polar angles ψ and ϕ are both measured counterclockwise from j-axis when we are facing the emerging beam.

In order to consider the problem of the corner reflector we may assume the aperture to be a certain reflector and the emerging beam to be the reflection of the incident beam impinging normally on the reflector.

Since our interest is in the distribution of the energy, we can normalize the amplitude such that in the case of a circular "perfect" mirror

the central intensity $I_o \equiv |U(0,0)|^2$ is unity. This yields

$$A(P) = \frac{1}{\pi a^2} \sum_{n=1}^{6} \gamma^n \int_0^a \int_{(n-1)\pi/3}^{n\pi/3} e^{-ikow\cos(\phi-\psi)} \rho d\rho d\phi \tag{7}$$

where A(P) is the normalized complex amplitude of the diffraction and γ^n is the normalized complex amplitude of the n-th sextant.

To evaluate the integral in Eq. (7), we use the formulas[9]

$$\cos(z\cos\theta) = J_o(z) + 2\sum_{k=1}^{\infty}(-)^k J_{2k}(z)\cos(2k\theta),$$

$$\sin(z\cos\theta) = 2\sum_{k=0}^{\infty}(-)^k J_{2k+1}(z)\cos[(2k+1)\theta],$$

where $J_{2k}(z)$ are the Bessel functions, to separate the radial and angular parts in the integral.[10] After evaluating the angular part, we obtain

$$A(P) = \frac{1}{\pi x^2}\sum_{n=1}^{6}\gamma^n\int_o^x y\,dy\{\frac{\pi}{3}J_o(y)$$

$$+ 4\sum_{\ell=1}^{\infty}\frac{(-i)^\ell}{\ell}J_\ell(y)\sin\frac{\ell\pi}{6}\cos[\ell(\frac{n\pi}{3}-\psi-\frac{\pi}{6})]\} \tag{8}$$

where $x = kaw$, $y = kow$.

It is known that

$$\int_o^x y\,J_o(y)\,dy = xJ_1(x), \tag{9}$$

and the second integral which involves higher orders of the Bessel functions

can be expressed in terms of the Bessel functions or in a power series of x. In either case the series converges rather quickly, and has the form[9]

$$\int_o^x y\, J_\ell(y)\, dy = 2\ell x \sum_{m=0}^{\infty} \frac{(\ell + 2m + 1)}{(\ell + 2m + 2)(\ell + 2m)}\, J_{\ell + 2m + 1}(x) \tag{10}$$

or

$$\int_o^x y J_\ell(y)\, dy = 4\left(\frac{x}{2}\right)^{\ell+2} \sum_{m=0}^{\infty} \frac{(-x^2/4)^m}{(\ell + 2m + 2)(m!)(\ell + m)!} \tag{11}$$

Since the integral is well-determined, we can, for short, define a new function $F_\ell(x)$ for $\ell \geq 1$ as:

$$F_\ell(x) \equiv \frac{1}{\ell x^2} \int_o^x y\, J_\ell(y)\, dy\ . \tag{12}$$

Then Eq. (3) can be rewritten as:

$$A(P) = \frac{2J_1(x)}{x} \sum_{n=1}^{6} \frac{\gamma^n}{6} + \frac{4}{\pi} \sum_{\ell=1}^{\infty} (-i)^\ell\, F_\ell(x)\, \sin\frac{\ell\pi}{6} \sum_{n=1}^{6} \gamma^n \cos\left[\ell\left(\frac{n\pi}{3} - \psi - \frac{\pi}{6}\right)\right]. \tag{13}$$

In the case of a "perfect" mirror, all γ^n's are equal to unity (omitting the common phase). Then $\sum_{n=1}^{6} \gamma^n/6 = 1$ plus the indentity

$$\sin\frac{\ell\pi}{6} \sum_{n=1}^{6} \cos\left[\ell\left(\frac{n\pi}{3} - \alpha\right)\right] \equiv 0$$

for all ℓ and α, reduces Eq.(13) to the well-known diffraction pattern resulting from a circular aperture,

$$A(P) = \frac{2J_1(kaw)}{kaw}\ .$$

This discussion has been for a single polarization. In general, (and for the corner reflector in particular) the polarization from each of the sextants may not be the same. Since beams of orthogonal polarization do not interfere, we may calculate the diffraction pattern due to each polarization, calculate the intensities due to each polarization, and then add the intensities. Although this may be done for a resolution into any pair of orthogonal polarization states, we will find it convenient to consider orthogonal linear polarizations.

IV. DIFFRACTION PATTERNS AS A FUNCTION OF THE REFLECTING SURFACE

In Section II we have derived the expressions of the normalized complex amplitudes for two orthogonal polarization states resulting from an incident linearly polarized plane wave with uniform intensity. The coefficients ξ, η and ζ, first defined in Eq. (2) are indeed determined by the properties of the reflecting surfaces; and the reflecting surfaces may be, as far as the corner reflector is concerned, glass-metal, glass-air or air-metal interface.

Since the light in orthogonal polarization states do not interfere, we will treat each of the outgoing polarizations separately. First we substitute the value of γ_p^n and γ_s^n obtained from Eq. (4) into Eq. (13) and then sum over n from 1 to 6. After somewhat lengthy algebraic calculations we obtain the expression of the normalized amplitude for both polarizations

$$A_p(x,\psi,\theta) = \xi G_0(x) + \eta G_1(x,\psi;\theta) \tag{14}$$

$$A_s(x,\psi;\theta) = \zeta G_2(x,\psi) + \eta G_3(x,\psi;\theta), \tag{15}$$

where

$$G_0(x) \quad \frac{2J_1(x)}{x} \tag{16}$$

$$G_1(x,\psi;\theta) \equiv \frac{(6)^{\frac{3}{2}}}{\pi} \sum_{\ell=1}^{2} \sum_{m=0}^{\infty} (-)^{m+1} F_{2\ell+6m}(x) \cos[(2\ell+6m)\psi + (-)^{\ell} 2\theta] \tag{17}$$

$$G_2(x,\psi) \equiv \frac{24}{\pi} \sum_{m=0}^{\infty} (-)^{m+1} F_{3+6m}(x) \sin(3+6m)\psi \tag{18}$$

$$G_3(x,\psi;\theta) \equiv \frac{(6)^{\frac{3}{2}}}{\pi} \sum_{\ell=1}^{2} \sum_{m=0}^{\infty} (-)^{m+\ell-1} F_{2\ell+6m}(x) \sin[(2\ell+6m)\psi + (-)^{\ell} 2\theta]. \tag{19}$$

It is interesting to note that the basic diffraction pattern of a corner reflector depends solely on four functions regardless of the property of the

surface. The difference in the properties of the reflecting surfaces affects only the strengths and the relative phases of these four functions.

Now we consider the energy which lies within a given angular radius from the center of the beam. Let $L(w_o)$ denote the fraction of the total energy which lies within an angular radius w_o. Then we obtain [11]

$$L(w_o) = \frac{\pi a^2}{\lambda^2} \int_0^{2\pi} \int_0^{w_o} I(w,\psi;\theta)\, w\, dw\, d\psi \quad , \tag{20}$$

where $\lambda = 2\pi/k$ is the wavelength of the light. The intensity is given by

$$I(w,\psi;\theta) = |A_p(x,\psi;\theta)|^2 + |A_s(x,\psi;\theta)|^2 \tag{21}$$

where $x = kaw$ as before. Using Eqs. (14) and (15), we get

$$\begin{aligned} I(w,\psi;\theta) = {} & |\xi|^2 G_o^2(x) + (\xi\eta^* + \xi^*\eta) G_o(x) G_1(x,\psi;\theta) + |\eta|^2 G_1^2(x,\psi;\theta) \\ & + |\zeta|^2 G_2^2(x,\psi) + (\zeta\eta^* + \zeta^*\eta) G_2(x,\psi) G_3(x,\psi;\theta) + |\eta|^2 G_3^2(x,\psi;\theta). \end{aligned} \tag{22}$$

Noting that the cross terms in $I(w,\psi;\theta)$ vanish after the angular integration over ψ, we may evaluate the angular part for each term and obtain

$$\begin{aligned} L(w_o) = {} & 2|\xi|^2 \int_0^x \frac{J_1^2(x)}{x}\, dx + \frac{108}{\pi^2} |\eta|^2 \sum_{\ell=1}^{2} \sum_{m=0}^{\infty} \int_0^{x_o} F_{2\ell+6m}^2(x)\, x\, dx \\ & + \frac{144}{\pi^2} |\zeta|^2 \sum_{m=0}^{\infty} \int_0^{x_o} F_{3+6m}^2(x)\, x\, dx. \end{aligned} \tag{23}$$

The energy within the first zero of the Airy pattern is given by $L(w_o)$ when $x_o = 3.83$ (or $w_o = 3.83/ka$) where the first zero of the Airy pattern occurs. Evaluating Eq. (23) numerically with that argument we obtain

$$L(w_o) = 0.840\, |\xi|^2 + 0.415\, |\eta|^2 + 0.056\, |\zeta|^2. \tag{24}$$

If we also consider the effect of absorption by the back surfaces we can denote the ratio of the total output energy to the total input energy by R and we have

$$R \equiv \frac{1}{6} \sum_{n=1}^{6} \underset{\sim}{u}^{\dagger} \underset{\sim}{C}^{n\dagger} \underset{\sim}{C}^{n} \underset{\sim}{u} / (\underset{\sim}{u}^{\dagger} \underset{\sim}{u})$$

$$= |\xi|^2 + 2|\eta|^2 + |\zeta|^2. \qquad (25)$$

As a simple illustration, let us consider the values of the coefficients ξ, η and ζ when the reflecting surface of a corner reflector acts as a "perfect" mirror. This ideal condition can be sufficiently described physically by the condition that the electric field which is parallel to the mirror surface vanishes, but the electric field which is perpendicular to the mirror surface remains unchanged. Then, it follows that $\rho_p = \rho_s = 1$ and $\delta_p = 0$, $\delta_s = \pi$ or in other words $r_p + r_s = 0$ and $r_p - r_s = 2$.

Substituting these values into Eq. (2), we obtain

$$\xi = 1 \text{ and } \eta = \xi = 0.$$

This result reduces Eqs. (14) and (15) to what we expect from a circular aperture, that is

$$A_p(x,\psi;\theta) = \frac{2J_1(x)}{x} \text{ and } A_s(x,\psi;\theta) = 0 .$$

Thus a corner reflector whose back surfaces act as a "perfect" mirror has the same diffraction pattern as a "perfect" flat circular mirror.

V. EXPECTED PATTERNS FROM CORNER REFLECTORS COATED WITH ALUMINUM, SILVER, UNCOATED, AND OPEN CORNER REFLECTORS

Since the diffraction pattern of a corner reflector is a linear combination of the four G-functions, we need only evaluate the coefficients ξ, η and ζ of different reflecting surfaces. We assume the wavelength of the light to be 6943 Å which is the value for a ruby laser. We have considered the cases of (1) an open corner reflector using the silver or the aluminum as the reflecting surfaces, (2) a solid corner reflector coated with the silver or the aluminum, and (3) an uncoated solid corner reflector. In all cases the index of refraction of the solid corner is assumed to be 1.45. The complex index of refraction of the metals was taken from Schulz and Tangherlini[12].

We have found that $|\eta|^2$ and $|\zeta|^2$ for the cases (1) and (2) are negligibly small (less than 1% of $|\xi|^2$). The energy ratios R are 95% and 70% for silver and aluminum, respectively, in case (1) and 92% and 61% in case (2).

For an uncoated solid corner $|\eta|^2$ and $|\zeta|^2$ are comparable with $|\xi|^2$. Although the energy ratio R is 100% in this case, the energy within the first zero of Airy pattern is about 36%.

The diffraction pattern for the case of (1) or (2) is approximately an Airy pattern. The diffraction pattern of an uncoated corner reflector is, however, quite different. We have evaluated the analytic expressions in Eqs. (14), (15) and (22) for $\theta = 0°$ and plotted the iso-intensity contours at different intensities in Figs. 2, 3 and 4. The total pattern as well

as the two components of the mutually orthogonal polarization states are shown separately.

The contours show certain symmetries, such as $I_p(x,\psi;0) = I_p(x,-\psi;0) = I_p(x, \pi-\psi;0)$, $I_s(x,\psi;0) = I_s(x,-\psi;0)$ for two orthogonal polarizations, and $I(x,\psi;0) = I(x,-\psi;0)$ for the over all pattern. These symmetries are quite obvious in Eqs. (16), (17), (18) and (19).

The photographs of the diffraction pattern are shown in Figs. 5, 6, and 7 for comparison with the plots. The corner reflector has an aperture of one inch in diameter. The entrance face, contrary to the assumption in this report, did not have an anti-reflection coating. However, one notices a striking resemblance between the photographs and the plots.

VI. CONCLUSION AND THE COMMENT

In this study of the far field diffraction pattern of a corner reflector, we considered, among other things, mainly the energy concentration at the central region.

The purpose of this particular consideration was to investigate the possibility of ranging to the moon with an optical radar system on the ground and the corner reflectors on the moon[13]. Thus quantitative information on the concentration of the returning signal was the primary interest.

The diffraction pattern from a circular aperture illuminated uniformly by a plane wave contains about 84% of its energy within the angular radius of $1.22\ \lambda/d$, where d is the diameter of the aperture. The diffraction pattern from a corner reflector utilizing total internal reflection contains slightly less than half of the energy from a circular aperture within that angular radius. The central irradiance is, for the case of a corner reflector, about one-fourth of that from a circular aperture. It is because the polarization effect manifests itself to a greater extent in the total internal reflection. There is little tendency that the field at points far away from the central region would be cancelled as it would be in the case of circular apertures. The consequence is a greater spread of energy. Coating the back surfaces of the corner reflector with metals would generally improve the performance in the sense that more energy would tend to concentrate in the central region. But the absorption of the light by the metal would reduce the returning intensity. The light entering a corner reflector has to be reflected three times before emerging, thus the desirability of high reflectance at the reflecting interface is greatly increased.

The particular geometry of the corner reflector predetermines the basic structure of its diffraction pattern as a combination of four functions. The different optical constants of the different reflecting interfaces provide merely the different coefficients for each of these four functions, namely ξ, η, and ζ.

Higher values of η and ζ would cause a wider spread of optical energy because the functions of which η and ζ are the coefficients consist of Bessel functions of higher order divided by their argument. A Bessel function reaches its largest value when the argument is roughly equal to its order; therefore, under the condition that $|\xi| \approx |\eta| \approx |\zeta|$ the diffraction field does not become small compared to the field strength at the central direction except when the angular direction is some distance away from the central direction. It is necessary that $|\eta| << |\xi|$ and $|\zeta| << |\xi|$ in order to reduce the spread of energy by diffraction.

A corner reflector whose back surfaces are coated with metal such as silver or aluminum satisfies the condition that $|\eta|$ and $|\zeta|$ are much smaller than $|\xi|$. Although it appears that such a corner reflector behaves roughly as an ideal reflector, its application to the optimization of return signal for the lunar ranging experiment is not straight forward. The extreme temperature gradients and the direct exposure to solar radiation in the actual lunar environment make the optimization of return signal a problem of a different nature which will not be discussed in this report.

FOOTNOTES

1. A. I. Mahan, J. Opt. Soc. Am., 35, 623 (1945); also A. I. Mahan and E. E. Price, J. Opt. Soc. Am., 40, 664 (1950).

2. E. R. Peck, J. Opt. Soc. Am., 52, 253 (1962).

3. M. M. Rao, Thesis, Department of Optics, University of Rochester, Rochester, New York, 1963.

4. P. Rabinowitz, S. F. Jacobs, T. Shultz, and G. Gould, J. Opt. Soc. Am., 52, 452 (1962).

5. P. R. Yoder, Jr., J. Opt. Soc. Am., 48, 496 (1958).

6. R. C. Spender, Report 433, Radiation Laboratory, M.I.T. (1944).

7. C. O. Alley, R. F. Chang, D. G. Currie, J. V. Mullendore, S. K. Poultney, J. D. Rayner, E. C. Silverberg, C. A. Steggerda, H. H. Plotkin, W. Williams, B. Warner, H. Richardson, and B. W. Bopp, Science, 167, 368 (1970).

C. O. Alley, R. F. Chang, D. G. Currie, S. K. Poultney, P. L. Bender, R. H. Dicke, D. T. Wilkinson, J. E. Faller, W. M. Kaula, G. J. F. MacDonald, J. D. Mulholland, H. H. Plotkin, W. Carrion, and E. J. Wampler, Science, 167, 458 (1970).

C. O. Alley, P. L. Bender, R. F. Chang, D. G. Currie, R. H. Dicke, J. E. Faller, W. M. Kaula, G. J. F. MacDonald, J. D. Mulholland, H. H. Plotkin, S. K. Poultney, D. T. Wilkinson, Irvin Winer, Walter Carrion, Tom Johnson, Paul Spadin, Lloyd Robinson, E. Joseph Wampler, Donald Wieber, E. C. Silverberg, C. A. Steggerda, J. V. Mullendore, J. D. Rayner, W. Williams, Brian Warner, Harvey Richardson, and B. W. Bopp, Apollo 11 Preliminary Science Report, SP-214, 163 (1969).

J. E. Faller, Irving Winer, Walter Carrion, Thomas S. Johnson, Paul Spadin, Lloyd Robinson, E. J. Wampler, and Donald Wieber, Science, 166, 99 (1969).

8. M. Born and E. Wolf, Principles of Optics, 2nd revised edition, p. 395 (MacMillan Company, New York, 1964).

9. Abramowitz and Stegun, Handbook of Mathematical Functions, 1965 (Dover, New York).

10. A. I. Mahan, C V. Bitterli, and S. M. Cannon, J. Opt. Soc. Am., 54, 721 (1964).

11. See Ref. 8, p. 398.

12. L. G. Schulz and F. R. Tangherlini, J. Opt. Soc. Am., 44, 362 (1954); and L. G. Schulz, J. Opt. Soc. Am., 44, 357 (1954).

13. C. O. Alley, P. L. Bender, R. H. Dicke, J. E. Faller, P. E. Franken, H. H. Plotkin, and D. A. Wilkinson, Journal of Geophysical Research, 70, 2267 (1965).

FIGURE CAPTIONS

Fig. 1 Front view of a corner reflector with a circular face is divided into six sections labeled by numbers 1 through 6. The projections of the real back edges and their images are indicated by the solid and dashed lines, respectively. The coordinate system is defined by the unit vectors $\hat{i}$ and $\hat{j}$.

Fig. 2 The iso-intensity contours of the total diffraction pattern are shown at three different intensities for $\theta = 0°$ in the polar coordinate. A quartz solid corner reflector (n=1.45) is assumed in the calculation. The contours at 50%, 10%, and 2% of the center intensity $I(0,\psi;0°)$ are shown by ————, ---------, and -·-·-·-· , respectively. The contour of the first zero of The Airy pattern is shown by the dotted line ..... for comparison.

Fig. 3 The iso-intensity contours of the diffraction pattern whose polarization is the same as that of the incident light.

Fig. 4 The iso-intensity contours of the orthogonal polarization. Notice that the 50% line is not present.

Fig. 5 The photograph of the total diffraction pattern from a quartz solid corner reflector without an anti-reflection coating.

FIGURE CAPTIONS

Fig. 6. The photograph of the component of the pattern having the original polarization.

Fig. 7 The photograph of the component of the pattern having the orthogonal polarization.

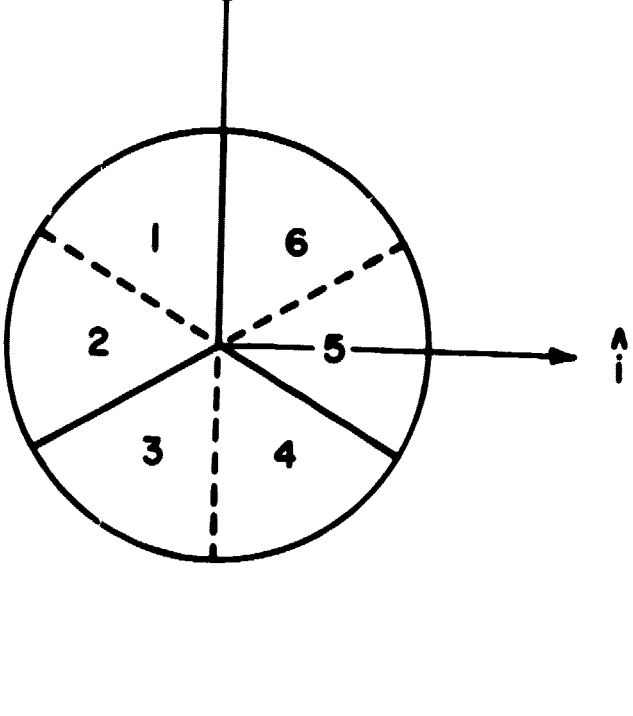

Figure 1

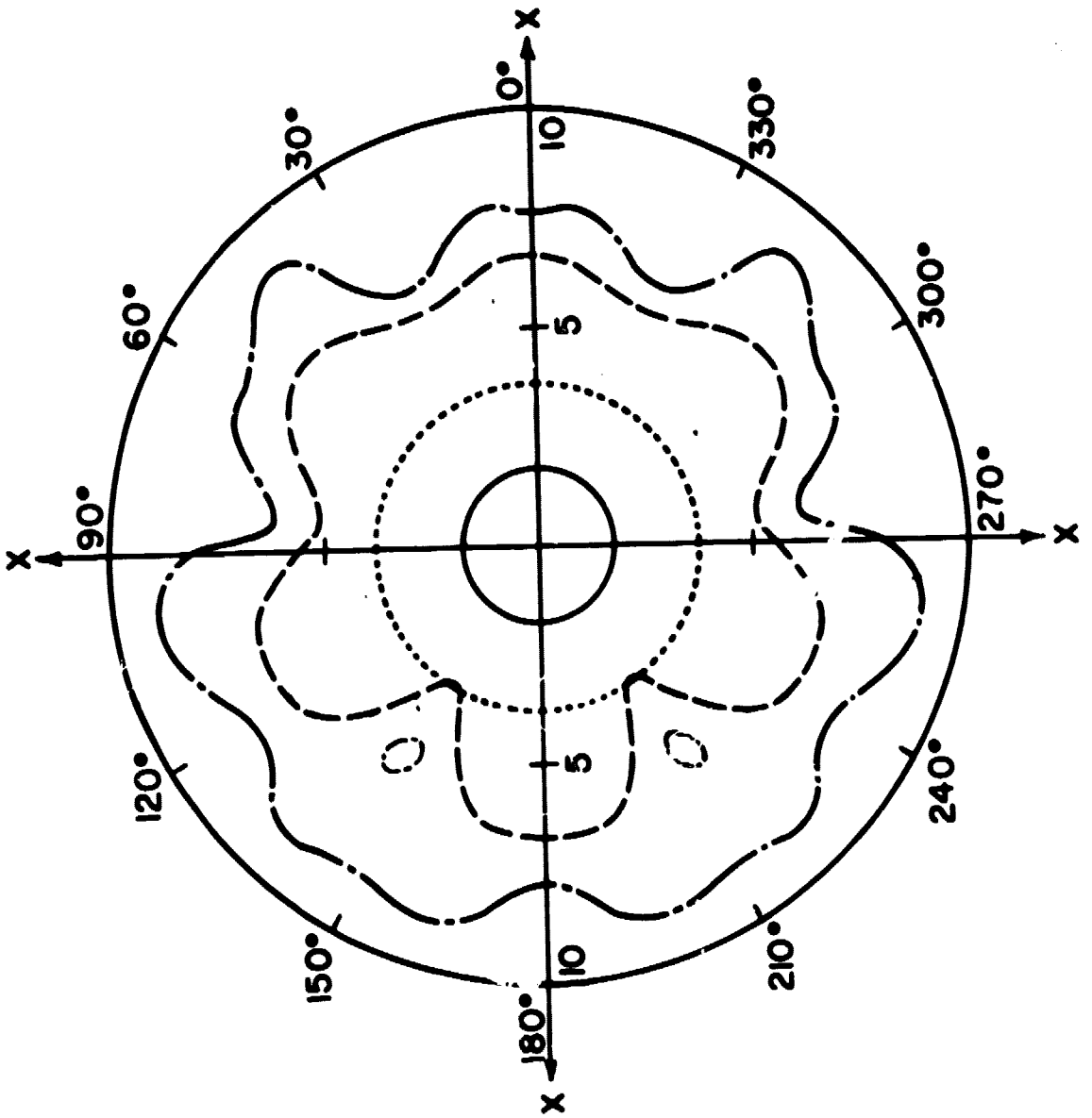

Figure 2

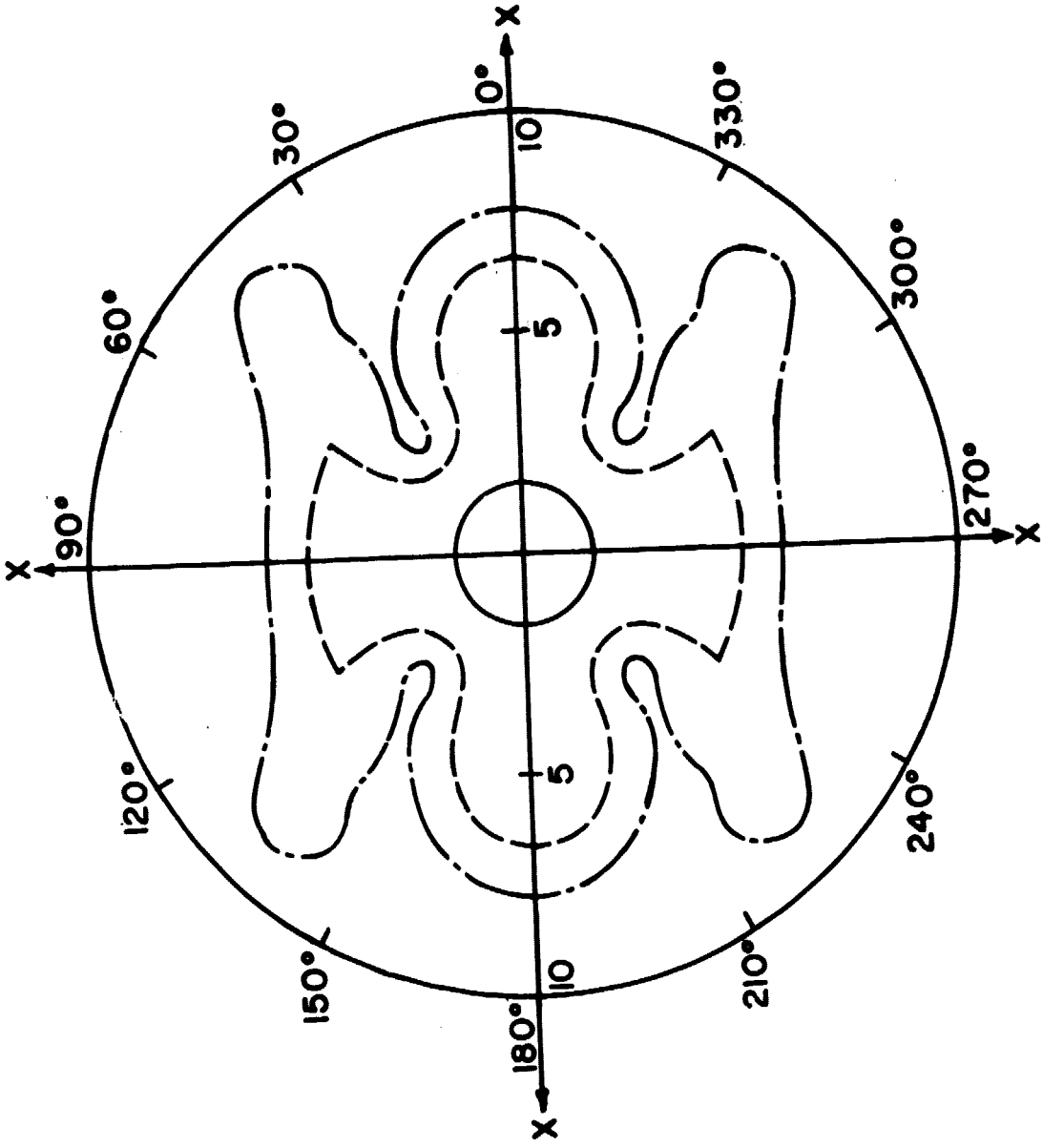

Figure 3

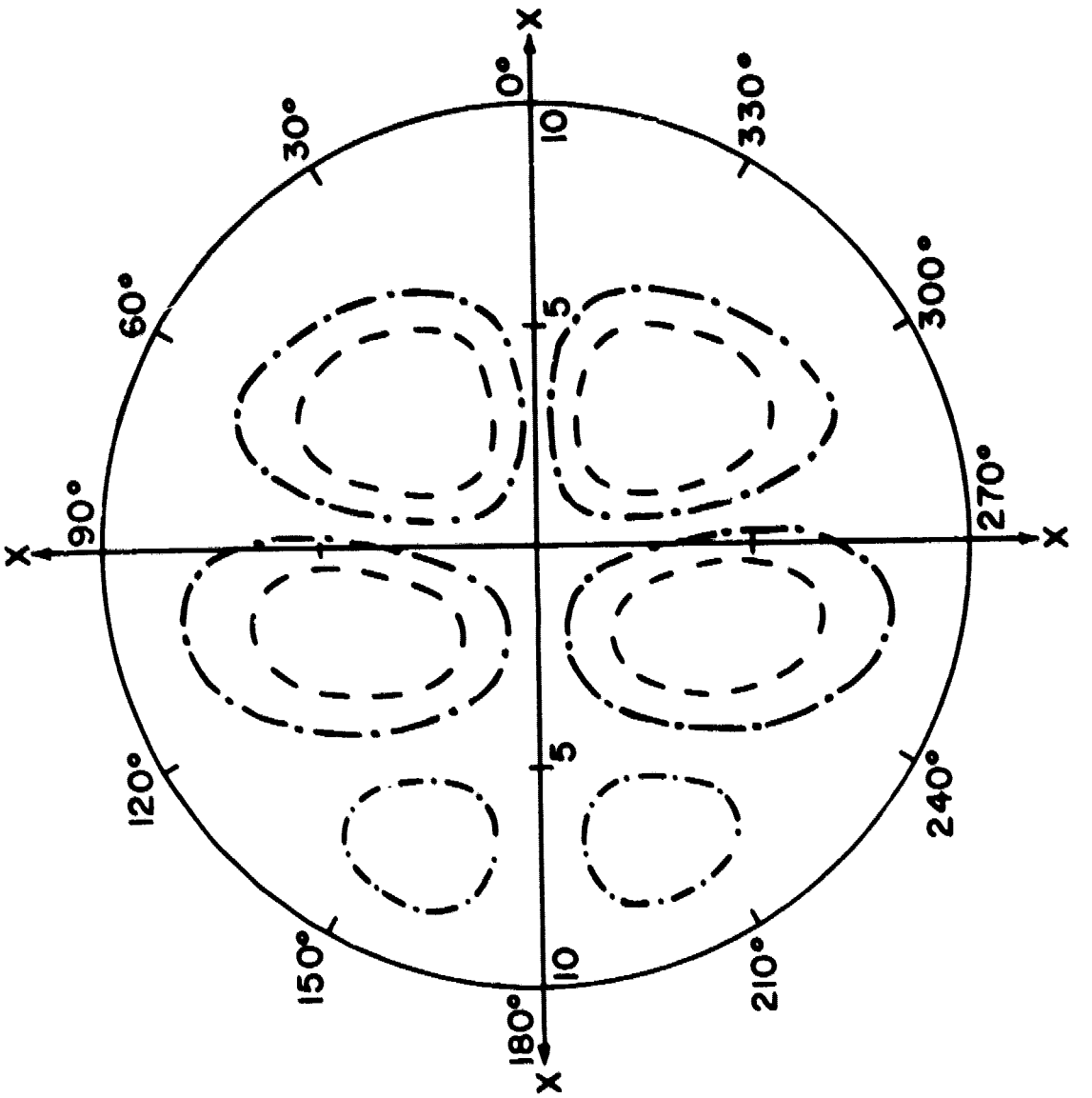

Figure 4

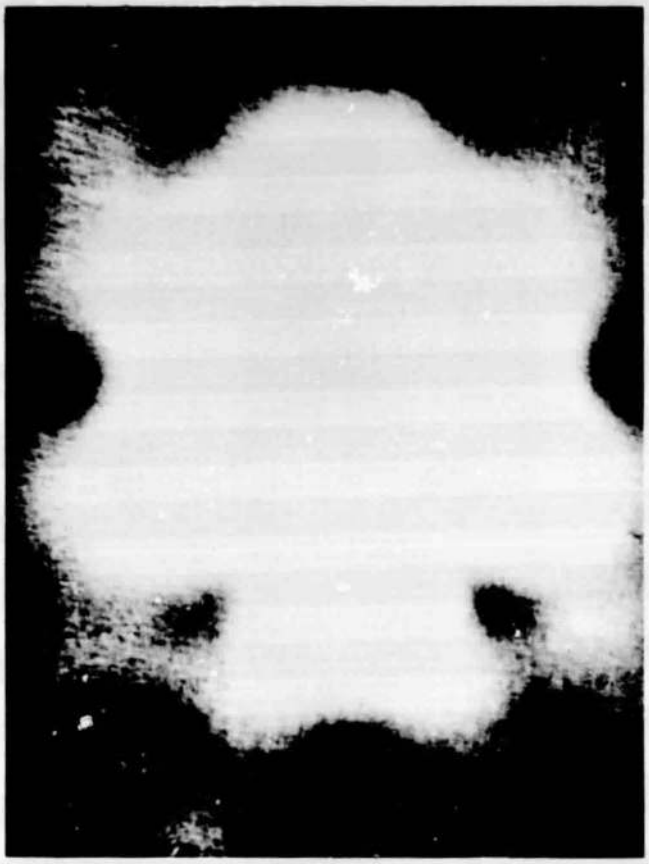

Figure 5

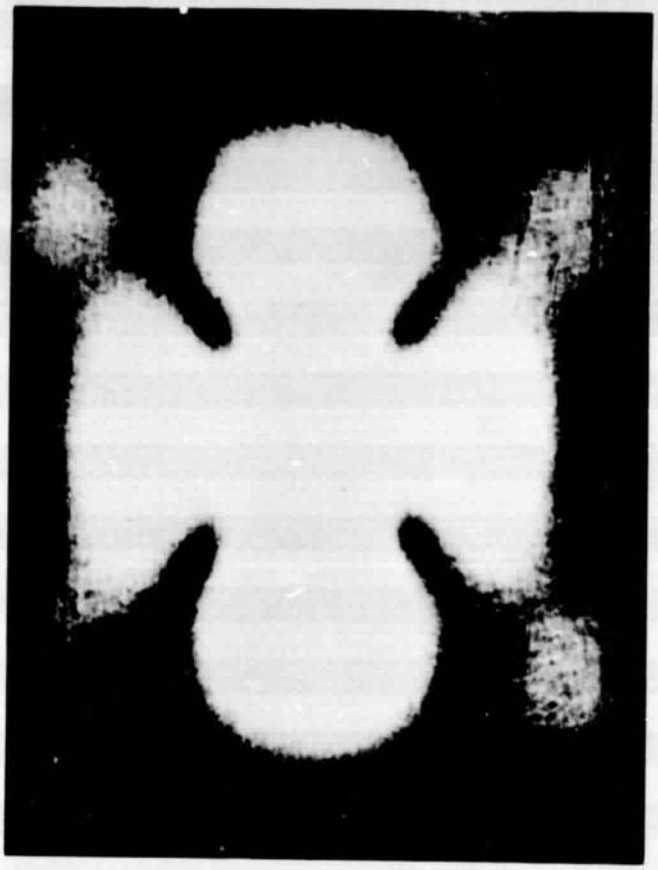

Figure 6

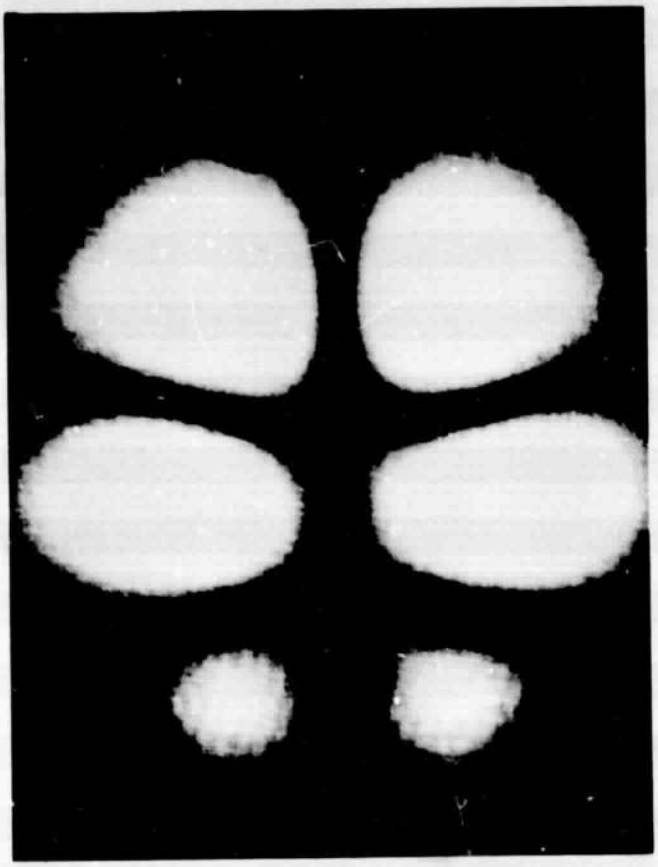

Figure 7

TABLE CAPTIONS

Table I: The Coefficients of the Transformation Matrices For the Six Sectors.

n	f_n	g_n	h_n
1	1	1	1
2	0	-1	-2
3	-1	1	1
4	1	-1	1
5	0	1	-2
6	-1	-1	1

TABLE I

ACKNOWLEDGMENT

The authors wish to acknowledge the assistance of George Hertzlinger in portions of the computer programming.